Pion-nucleus optical potential valid up to the Δ-resonance region

L. J. Abu-Raddad*
Research Center for Nuclear Physics, Osaka University, 10-1 Mihogaoka, Ibaraki, Osaka 567-0047, Japan
(Received 4 July 2002; published 4 December 2002)

We present in this article an optical potential for the π-nucleus interaction that can be used in various studies involving π-nucleus channels. Based on earlier treatments of the low-energy π-nucleus optical potential, we have derived a potential expression applicable from threshold up to the Δ-resonance region. We extracted the impulse approximation form for this potential from the π-N scattering amplitude and then added to it kinematical and physical corrections. The kinematic corrections arise from transforming the impulse approximation expression from the π-N center of mass frame to the π-nucleus center of mass frame, while the physical corrections arise mostly from the many-body nature of the π-nucleus interaction. By taking advantage of the experimental progress in our knowledge of the π-N process, we have updated earlier treatments with parameters calculated from state-of-the-art experimental measurements.

DOI: 10.1103/PhysRevC.66.064601 PACS number(s): 25.80.Dj, 13.75.Gx, 24.10.Ht

I. INTRODUCTION

The purpose of this work is to provide a π-nucleus optical potential valid up to the Δ-resonance region that can be used in various studies involving the π-nucleus interaction. Specifically, we supply a potential that can provide an integral component in the analysis of several future and past experiments in pion photoproduction and electroproduction processes from nuclei at Thomas Jefferson National Accelerator Facility (Jefferson Lab) and Mainz [1–5]. Indeed, the personal motivation for this study is a study of the coherent pion photoproduction from nuclei in the Δ-resonance region [6,7].

The π-nucleus elastic scattering has enjoyed significant investigation from a variety of theoretical perspectives [8]. Our approach here is to extend the prominent work of Stricker, McManus and Carr (SMC) [9–12] on the low-energy π-nucleus optical potential to higher energies so that it covers the Δ-resonance region. Indeed, our treatment here follows closely the SMC analysis but extends their treatment to higher energies. We do so by first not using any low-energy approximation. Second, we invoke a fully covariant kinematics including the nucleus recoil. Third, we update their treatment by using *s*- and *p*-wave parameters calculated from state-of-the-art experimental measurements, and we keep these parameters intact by not attempting to change them to fit any specific data. Finally, we include terms that the SMC group ignored either because of their small effect at low energy or because of the fitting procedure which allowed them to absorb theses terms in the refitted parameters.

Bearing these facts in mind, in what follows we outline the formalism used to derive the optical potential. We begin from where the SMC work started by taking the elementary amplitude of the process $\pi N \rightarrow \pi N$ and using it, along with the impulse approximation, to develop the amplitude for the π-nucleus interaction. We arrive then at what is known as the impulse approximation form of the optical potential. Such a form, however, still lacks two classes of corrections: kinematical and physical ones. The kinematical ones arise from transforming the π-N elementary amplitude from the π-N center of mass (c.m.) frame to the π-nucleus c.m. system. The physical corrections, however, arise from the fact that the impulse approximation picture does not encompass distinct many-body interactions that appear only in the π-nucleus channel. These effects include multiple scattering, pion absorption, Pauli blocking, and Coulomb corrections. They are of second and higher orders in strength compared to the first-order expression given by the impulse approximation.

The paper has been organized as follows. In Sec. II, the optical potential is derived starting from the π-N elementary amplitude while the final form of the potential is presented in Sec. III. Next, a number of applications are discussed in Sec. IV, and various results are compared with experimental data. Finally, conclusions are drawn in Sec. V.

II. DERIVATION OF THE OPTICAL POTENTIAL

A. Pion-nucleon elementary process

The starting point for our derivation of the optical potential is the π-N scattering amplitude which is given by [9–12]

$$f_{\pi N}(\pi N \rightarrow \pi N) = b_0 + b_1 \mathbf{t}\cdot\boldsymbol{\tau} + (c_0 + c_1 \mathbf{t}\cdot\boldsymbol{\tau})\mathbf{k}.\mathbf{k}', \quad (1)$$

where $\mathbf{t}$ and $\boldsymbol{\tau}$ are the pion and nucleon isospin operators, $\mathbf{k}$ and $\mathbf{k}'$ are the incoming and outgoing pion momenta, b_0 and b_1 are the *s*-wave parameters while c_0 and c_1 are the *p*-wave parameters. In this expression the small spin-dependent term has been neglected [10].

The *s*- and *p*-wave parameters are determined from the phase shifts of the interaction according to a formalism sketched in Ref. [13]. In the earlier treatments [9–12], these parameters were determined initially from a phase-shift analysis performed by Rowe, Salomon, and Landau [14], but then were modified to obtain the best fit for the π-nucleus scattering and pionic atom data. Our treatment here differs in two respects: first, we extract the parameters from the state-of-the-art experimental measurements and phase-shift analysis of Arndt, Strakovsky, Workman, and Pavan from the Vir-

*Electronic address: laith@rcnp.osaka-u.ac.jp

 ©2002 The American Physical Society

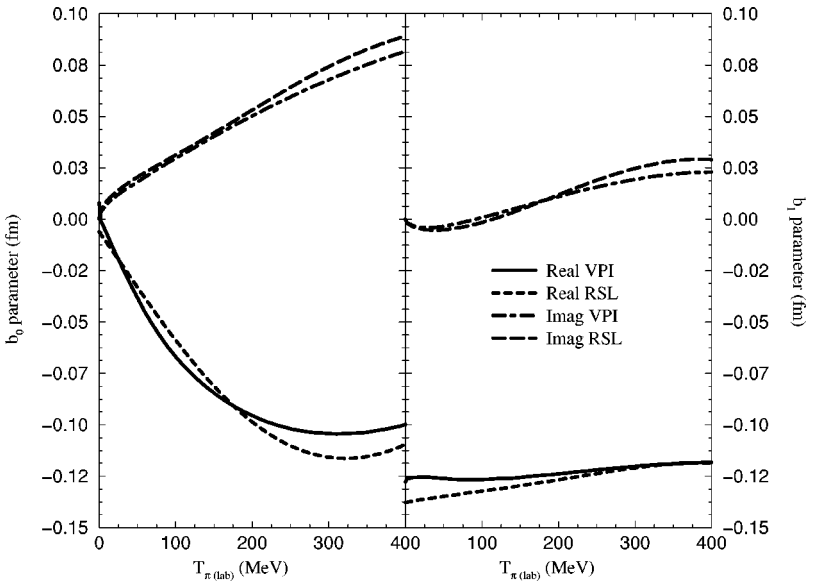

FIG. 1. The b_0 (left panel) and b_1 (right panel) *s*-wave elementary amplitude parameters as functions of the pion kinetic energy in the laboratory system $T_{\pi(\mathrm{lab})}$. The figure draws a comparison between parameters extracted from the state-of-the-art Arndt *et al.* (VPI) experimental measurements [15] and those extracted from the Rowe *et al.* (RSL) phase-shift analysis [14] more than 20 years earlier.

ginia Tech SAID program [15]. Second, we keep these parameters intact by not attempting to change them to fit any specific data. In doing so we have maintained the theoretical basis for the optical potential unblemished. This is particularly important in this work as these parameters dominate the optical potential in the Δ-resonance region.

Having extracted the *s*- and *p*-wave parameters from the phase-shift analysis of Arndt *et al.* (VPI), we compare them with those extracted using the Rowe *et al.* (RSL) phase shifts. Figures 1 and 2 show the b_0, b_1, c_0, and c_1 parameters as functions of the pion kinetic energy in the laboratory system. It is evident that the VPI and RSL results are comparable and that there are only small differences. This is indeed notable in light of the limited experimental measurements at pion momenta higher than 250 MeV at the time Rowe *et al.* published their results.

B. Kinematic corrections

After adopting the π-N amplitude of Eq. (1) in the π-N c.m. frame, the next step in the derivation is to transform the amplitude to the π-nucleus c.m. system. This is done using the relativistic potential theory of Kerman, McManus, and Thaler [16] which establishes a relationship between the π-N transition matrix (t) in the π-N c.m. frame and the π-N amplitude in the π-nucleus c.m. frame according to Ref. [17]:

$$\langle k',p'|t|k,p\rangle=(2\pi)^3\delta(\vec{k}'+\vec{p}'-\vec{k}-\vec{p})\mathcal{K}f_{\pi N}(k'_{\mathrm{c.m.}},k_{\mathrm{c.m.}}), \tag{2}$$

where k and p (k' and p') are the initial (final) pion and nucleon momenta in the π-nucleus c.m frame while $k_{\mathrm{c.m.}}$ and $k'_{\mathrm{c.m.}}$ are the initial and final pion momenta in the π-N c.m. system. $\mathcal{K}$ is some involved kinematic factor [10].

Next, we express the arguments of $f_{\pi N}(k'_{\mathrm{c.m.}},k_{\mathrm{c.m.}})$ in terms of the appropriate kinematical quantities in the π-nucleus c.m. frame. This is done using what is referred to as the ''angle transformation'' which relates the $k'_{\mathrm{c.m.}}$ and $k_{\mathrm{c.m.}}$ to the corresponding quantities in the π-nucleus c.m.

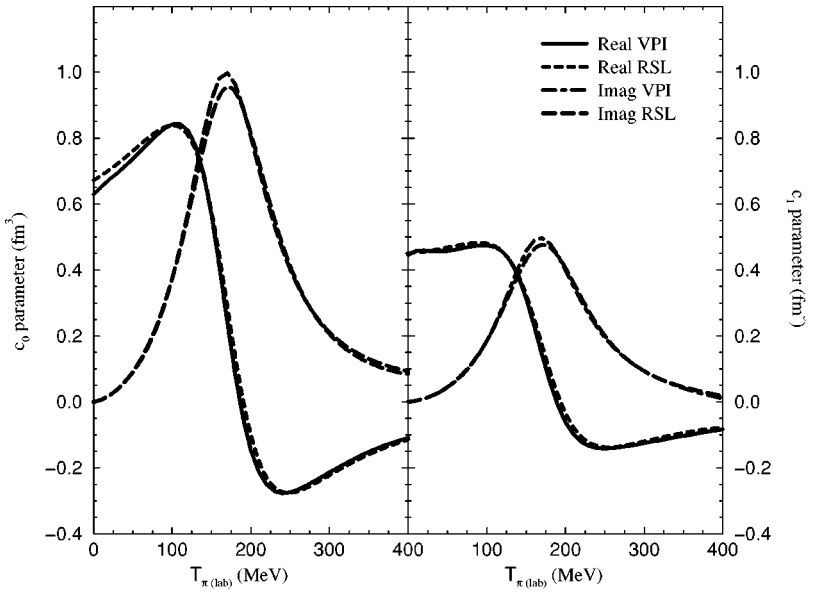

FIG. 2. The c_0 (left panel) and c_1 (right panel) *p*-wave elementary amplitude parameters as functions of the pion kinetic energy in the laboratory system $T_{\pi(\mathrm{lab})}$. The figure draws a comparison between parameters extracted from the state-of-the-art Arndt *et al.* (VPI) experimental measurements [15] and those extracted from the Rowe *et al.* (RSL) phase-shift analysis [14] more than 20 years earlier.

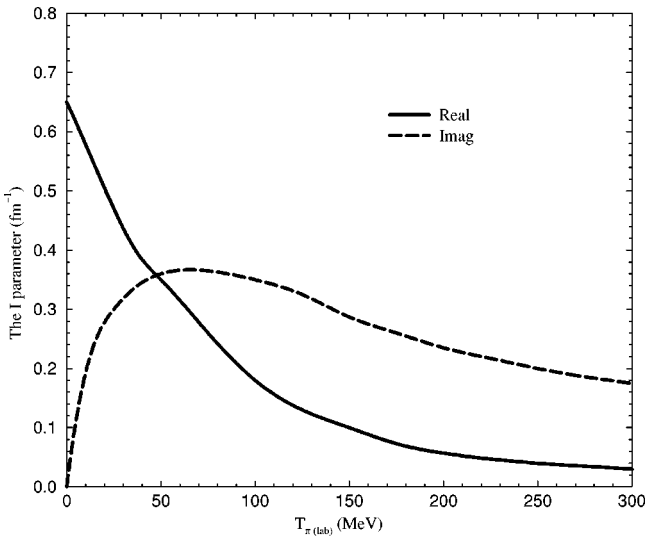

FIG. 3. The I parameter as a function of the pion kinetic energy in the laboratory system $T_{\pi(\mathrm{lab})}$. This quantity is necessary in the incorporation of multiple scattering corrections to the b_0 (s-wave) parameter.

system through a Lorentz transformation [10]. As a consequence of this boost, a term proportional to the dot product of nucleon momenta $\vec{p}\cdot\vec{p}'$, that is proportional to the kinetic energy density in the nucleus, is encountered. Using Thomas-Fermi approximation, it leads to the optical potential term $\tilde{K}(r)\sim c_0\rho^{5/3}(r)$, where $\rho(r)$ is the nuclear matter density. This term, although derived by Stricker-Bauer [10], was ignored in the SMC potential largely because its effect is absorbed in the parameter fitting. Since we have elected to preserve the physical basis of our parameters, this term must be included.

C. Multiple scattering corrections

By invoking the impulse approximation, the resultant form for the amplitude is then sandwiched between bound-nucleon states and the expression is summed over all occupied states of the nucleus. Hence, one obtains the π-nucleus interaction amplitude in momentum space. Taking the Fourier transform, we obtain the impulse approximation expression for the optical potential. This form still lacks physical corrections arising from many-body processes, which alter the scattering amplitude parameters such as b_0 and c_0 and add new terms to the optical potential. Thus, we incorporate the second-order multiple scattering corrections to the small (nearly zero) s-wave terms that play an important role only at low energies as the p-wave effect is still small in this energy regime. This correction was first calculated by Ericson and Ericson [18]. Here we adopt the formalism given by Krell and Ericson [19] which yields a term in the potential proportional to the nuclear density. Effectively, this correction shifts the b_0 parameter by a term proportional to $(b_0^2+2b_1^2)I$, where I is the so-called $1/r_{correlation}$ function calculated by Stricker-Bauer [10] and is shown in Fig. 3. At very low energy ($\leqslant$10 MeV) a good approximation for this function is $I=3k_F/2\pi$, where k_F is the nucleon Fermi momentum in the free gas model. In the SMC work [9–12], this constant value was used for I. It is clear in Fig. 3 that I falls rapidly and so this assumption is, in principle, not justified. Nonetheless, since they fitted their parameters, the effect of this correction is buried in the refitted value for b_0. We include this term in our study with its exact behavior as a function of energy.

The p-wave terms are the crucial ones in the Δ-resonance region and thus we include higher-order corrections by summing the multiple scattering series to all orders. This was first done by Ericson and Ericson [18] who concluded that this summation introduces a term of the form $\boldsymbol{\nabla}\cdot\mathcal{Q}(r)\boldsymbol{\nabla}$. This nonlocal form became to be known in the literature as the Ericson-Ericson effect which is analogous to the Lorentz-Lorenz effect in electrodynamics [20]. The exact form of the function $\mathcal{Q}(r)$ is a matter of dispute due to the method in which the multiple scattering series is summed and due to the nature of the assumed short-range correlations between nucleons. Here we follow the SMC methodology [9–12] of summing the series partially to all orders to obtain a term of the form

$$\frac{L(r)}{1+\frac{4\pi}{3}L(r)}+p_1x_1\acute{c}\rho(r), \tag{3}$$

where $L(r)$ includes contributions from the c_0 (p-wave) and absorption terms to be discussed in Sec. II D. The kinematic factors p_1 and x_1 are defined below. This term still lacks the inclusion of short-range correlations. Various studies have attempted to calculate these contributions under different assumptions [21,22]. They concluded that such correlations reduce the strength of this form through a parameter λ according to

$$\frac{L(r)}{1+\frac{4\pi}{3}\lambda L(r)}+p_1x_1\acute{c}\rho(r). \tag{4}$$

The value of λ is not precisely established. Nonetheless, there is an agreement that it is greater than one due to the finite range of the pion-nucleon interaction. Baym and Brown predicts a value of 1.6 or higher while Oset and Weise estimate it in the range of 1.2–1.6. Values in the range of 1.2–1.6 are common in the literature [9–12].

The second term $p_1x_1\acute{c}\rho(r)$ in Eq. (3) appears naturally in summing the multiple scattering series [10] but was not included in the SMC work because of its small contribution at low energy. However, this term is sizable in the Δ-resonance region as can be seen in Fig. 4 which displays the $\acute{c}$ parameter along with the dominant c_0 one.

D. Pion absorption corrections

Having included multiple scattering corrections, we are now in a a place to discuss pion absorption processes that generate the absorption terms in the optical potential. There are two types of such terms: the first one arises from the fact that there are many open inelastic channels in the π-nucleus interaction such as nucleon knock-out. Accordingly, a por-

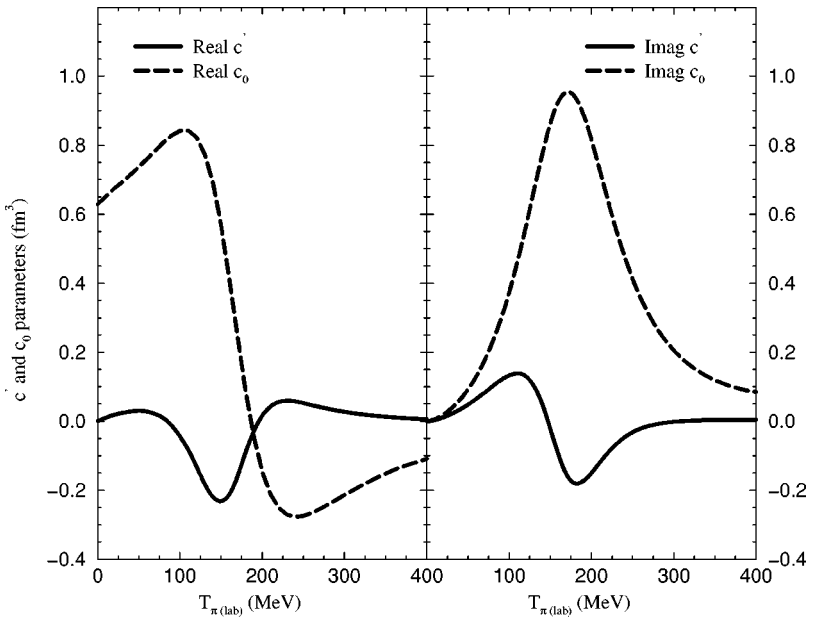

FIG. 4. The real parts (left panel) and the imaginary parts (right panel) of the $\acute{c}$ and c_0 parameters as functions of the pion kinetic energy in the laboratory system $T_{\pi(\mathrm{lab})}$. While small at low and high energies, the $\acute{c}$ parameter is considerable in the Δ-resonance region.

tion of the incoming flux is absorbed by these processes leading to an imaginary part in the potential. This kind of absorption is naturally included in the impulse-approximation form for the potential. The second type of absorption originates from many-body mechanisms such as two-nucleon absorption where the pion is scattered from one nucleon but then absorbed by another. This is in fact the dominant many-body absorption mechanism and has to be incorporated in the potential. The many-body absorption mechanisms are referred to as ''true absorption'' to distinguish them from the inelastic (type one) absorptions. Ironically, the Δ-resonance formation that drives strongly the elementary process $\pi N \rightarrow \pi N$, dampens it in the nuclear medium through absorption channels.

The two-nucleon absorption contribution is derived from the pion-two nucleon amplitude in analogous methodology to that of Sec. II A, but in the pion-two nucleon c.m. frame [18]. This introduces new scattering *s*- and *p*-wave parameters B_0, B_1, C_0, and C_1 such as those in Eq. (1). They can, as a matter of principle, be determined from the various amplitudes of the pion-two-nucleon systems including the reaction $\pi d \rightarrow NN$. However, it is difficult to disentangle the deuteron structure effects and thus we adopt the parameters as calculated theoretically for nuclear matter by Chai and Riska [23].

After establishing the pion-two nucleon amplitude, the expression is transformed to the π-nucleus c.m. system and the angle transformation is invoked to express the various kinematical quantities in the π-nucleus c.m. frame. In turn, this introduces further kinematic corrections such as those described in Sec. II B. The amplitude is then folded in the nucleus using the impulse approximation. Higher-order *p*-wave absorption terms are summed leading to an absorption contribution to the Ericson-Ericson nonlocal term [see Eq. (3)]. Figure 5 shows the B_0 and C_0 absorption parameters as a function of the pion kinetic energy in the laboratory system. The absorption isospin parameters B_1 and C_1 are very small and have been neglected in our formalism.

E. Pauli correction

Another alteration to the potential is the Pauli correction. Due to the Pauli principle, the number of available final states for the struck nucleon in the nuclear medium is reduced by Pauli blocking leading to this kind of correction. The effect can be treated approximately by reducing the imaginary parts of the parameters b_1, c_0, and c_1 by a factor Q that parametrizes the fraction of phase space available to the struck nucleon [10]. This correction has already been incorporated for the b_0 parameter in the calculation of the second-order correction. To be noted here that this effect does not, to a large extent, influence the imaginary parts of the absorptions parameters B_0, B_1, C_0, and C_1 as the nucleon gains a large value of momentum when the pion is absorbed.

The Q factor has been estimated for pions by Landau and McMillan [24] and is shown for completeness in Fig. 6. It is evident that at low energy, Q is vanishing as no states are available for the struck nucleon while it approaches the identity at higher energies as a large volume of phase space becomes available to the struck nucleon.

F. Coulomb corrections

An additional correction is the Coulomb one, stemming from the fact that the incoming charged pion (in π-nucleus scattering) is accelerated or decelerated depending on its charge, by the long-range Coulomb field of the nucleus before interacting through the short-range strong interaction. This correction shifts the value of kinetic energy at which the optical potential is evaluated to account for the acceleration or deceleration according to $T_{\pi(\mathrm{lab})} \rightarrow T_{\pi(\mathrm{lab})} - \varepsilon_\pi E_{Coul}$, where E_{Coul} is the value of the Coulomb field at the nuclear surface and ε_π is the pion charge. Figure 7 displays the E_{Coul} parameter as a function of the proton number Z of the nucleus. While this correction is very small for light nuclei and at low energies where the parameters vary slowly, it

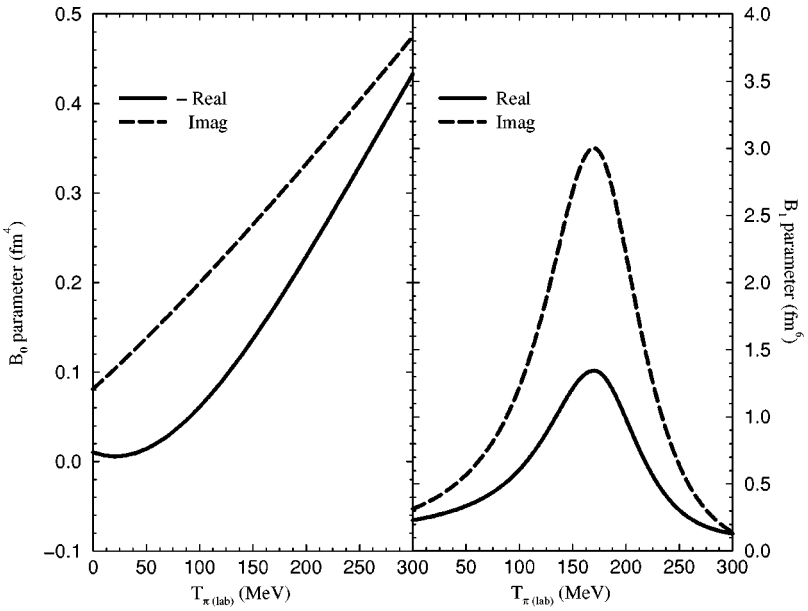

FIG. 5. The B_0 (left panel) and C_0 (right panel) absorption parameters as functions of the pion kinetic energy in the laboratory system $T_{\pi(\mathrm{lab})}$.

plays a significant role for heavy nuclei and specially at the Δ-resonance region where the parameters change rapidly.

III. OPTICAL POTENTIAL FORM

In implementing the above mentioned corrections, we arrive at a π-nucleus optical potential—applicable from threshold up to the Δ-resonance region—of the form

$$2\omega U = -4\pi\left[p_1 b(r) + p_2 B(r) - \boldsymbol{\nabla}\mathcal{Q}(r)\cdot\boldsymbol{\nabla} - \frac{1}{4}p_1 u_1 \nabla^2 c(r) - \frac{1}{4}p_2 u_2 \nabla^2 C(r) + p_1 y_1 \tilde{K}(r)\right], \tag{5}$$

where

$$b(r) = \overline{b_0}\rho(r) - \epsilon_\pi b_1 \delta\rho(r), \tag{6}$$

$$B(r) = B_0\rho^2(r) - \epsilon_\pi B_1 \rho(r)\,\delta\rho(r), \tag{7}$$

$$c(r) = c_0\rho(r) - \epsilon_\pi c_1 \delta\rho(r), \tag{8}$$

$$C(r) = C_0\rho^2(r) - \epsilon_\pi C_1 \rho(r)\,\delta\rho(r), \tag{9}$$

$$\mathcal{Q}(r) = \frac{L(r)}{1 + \frac{4\pi}{3}\lambda L(r)} + p_1 x_1 \acute{c}\rho(r), \tag{10}$$

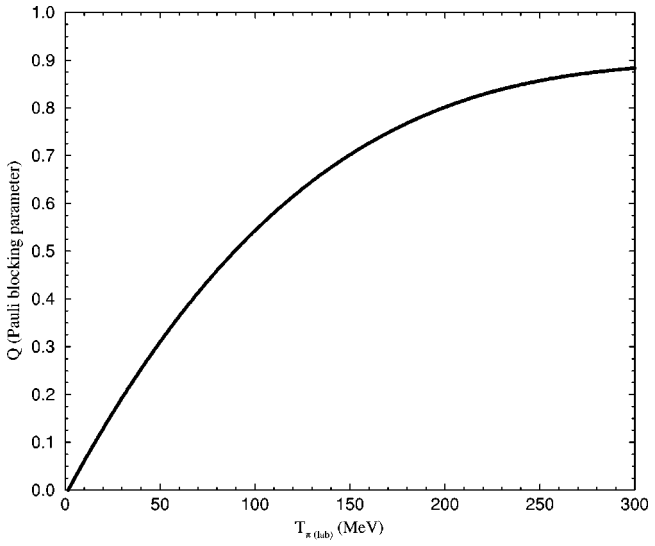

FIG. 6. The Pauli blocking parameter Q as a function of the pion kinetic energy in the laboratory system $T_{\pi(\mathrm{lab})}$. This parameter reduces the imaginary parts of the parameters b_1, c_0, and c_1 by a factor of Q to account for the reduction in bound-nucleon available phase space.

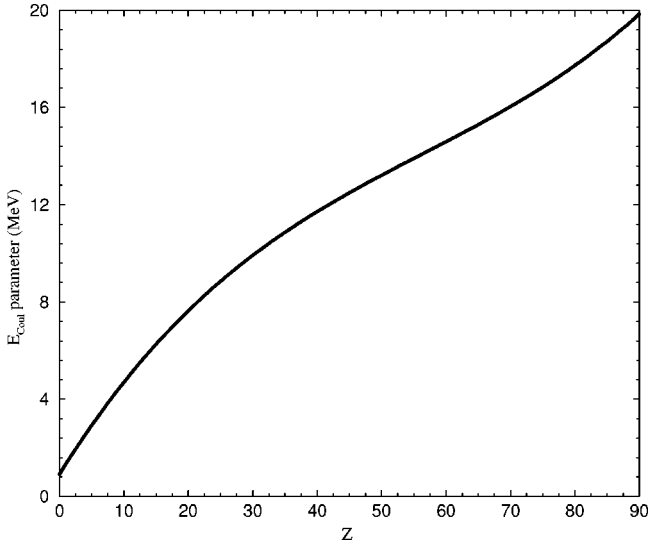

FIG. 7. The Coulomb energy correction parameter E_{Coul} as a function of the nuclear proton number Z. This correction shifts the value of the pion kinetic energy in the laboratory system $T_{\pi(\mathrm{lab})}$ at which the optical potential is evaluated to account for the acceleration or deceleration of the incoming charged pion, before it feels the short-range strong interaction of the nucleus.

$$L(r)=p_1x_1c(r)+p_2x_2C(r), \tag{11}$$

$$\tilde{K}(r)=\frac{3}{5}\left(\frac{3\pi^2}{2}\right)^{2/3}c_0\rho^{5/3}(r), \tag{12}$$

and with

$$\overline{b_0}=b_0-p_1\frac{A-1}{A}(b_0^2+2b_1^2)I, \tag{13}$$

$$\acute{c}=p_1x_1\frac{1}{3}k_o^2(c_0^2+2c_1^2)I. \tag{14}$$

In the above expressions, the set $\{p_1,u_1,x_1,$ and $y_1\}$ represents various kinematic factors in the effective π-N system (pion-nucleon mechanisms) that are determined from the set of equations

$$p_1=\left(\frac{E_N+\omega}{E_A+\omega}\right)\left(\frac{E_A}{E_N}\right), \tag{15a}$$

$$u_1=2(D_1+D_1^2), \tag{15b}$$

$$x_1=(1+D_1)^2, \tag{15c}$$

$$y_1=D_1^2. \tag{15d}$$

Here

$$D_1=\frac{F_1}{E_N+\omega}, \tag{16a}$$

$$F_1=\gamma_1\left(\frac{\gamma_1}{\gamma_1+1}\vec{\beta}_1\cdot\vec{k}-\omega\right), \tag{16b}$$

$$\gamma_1=\frac{1}{\sqrt{1-\beta_1^2}}, \tag{16c}$$

$$\beta_1=\frac{k}{E_N+\omega}\left(1-\frac{1}{A}\right), \tag{16d}$$

$$\vec{\beta}_1\cdot\vec{k}=\beta_1k. \tag{16e}$$

In these expressions, A is the atomic number, ω and k are the pion energy and momentum, while E_A is the nucleus energy and E_N is the nucleus energy per nucleon. These kinematic quantities are in the π-nucleus c.m. frame. Note the appearance of the Lorentz transformation parameters β_1 and γ_1 in these expressions. This is a result of the angle transformation described in Sec. II B.

The set $\{p_2,u_2,$ and $x_2\}$ represents kinematic factors in the π-$2N$ system (pion-two nucleon mechanisms):

$$p_2=\left(\frac{2E_N+\omega}{E_A+\omega}\right)\left(\frac{E_A}{2E_N}\right), \tag{17a}$$

$$u_2=2(D_2+D_2^2), \tag{17b}$$

$$x_2=(1+D_2)^2. \tag{17c}$$

where

$$D_2=\frac{F_2}{2E_N+\omega}, \tag{18a}$$

$$F_2=\gamma_2\left(\frac{\gamma_2}{\gamma_2+1}\vec{\beta}_2\cdot\vec{k}-\omega_2\right), \tag{18b}$$

$$\gamma_2=\frac{1}{\sqrt{1-\beta_2^2}}, \tag{18c}$$

$$\beta_2=\frac{k}{2E_N+\omega}\left(1-\frac{2}{A}\right), \tag{18d}$$

$$\vec{\beta}_2\cdot\vec{k}=\beta_2k. \tag{18e}$$

Note the appearance of the factor 2 in many terms in these pion-two-nucleon quantities as opposed to the factor 1 in the corresponding quantities in the pion-nucleon system.

The set of parameters $\{b_0,b_1,c_0,$ and $c_1\}$ originates from the $\pi N\rightarrow\pi N$ elementary amplitudes while all other parameters, excluding kinematic factors, have their origin in the second- and higher-order corrections to the optical potential. Nuclear effects enter the optical potential through the nuclear density $\rho(r)$, and through the neutron-proton density difference (isovector density) $\delta\rho(r)$. These densities were calculated using a mean-field approximation to the quantum hadrodynamics model (QHD) of Walecka [25]. Finally, k_o is the pion laboratory momentum, λ is the Ericson-Ericson effect parameter, and I is the $1/r_{correlation}$ function (Sec. II C). The B and C parameters arise from true pion absorption (Sec. II D).

IV. RESULTS AND DISCUSSION

Having establsihed the optical potential, it is appropriate to test it for a variety of nuclei and at various energies from threshold up to the Δ-resonance region. Figure 8 shows the differential cross section of π^+ elastic scattering from ^{208}Pb at pion laboratory kinetic energy of 30.7 MeV and as a function of the scattering angle in the c.m. frame. Experimental data are obtained from Ref. [26]. In the left panel of the figure, we display the calculated cross section using our optical potential (solid-line) and comapre it with the data. It is evident that the potential lacks some strength as it underestimates the data. This is in fact the well-known problem of missing s-wave attraction at low energy [9–12]. Indeed, this missing strength was one of the main reasons that caused the SMC group to refit the parameters enhancing the s-wave attraction. We also show in the same panel the significantly improved result with an enhanced s-wave attraction. The physics behind this enhancement is not clear, but likely due to some many-body effect not included in the optical potential. The effect is specially pronounced for heavy nuclei such as ^{208}Pb and does not appear to be as important for light ones as can be seen in Fig. 9 where we plot the differential cross

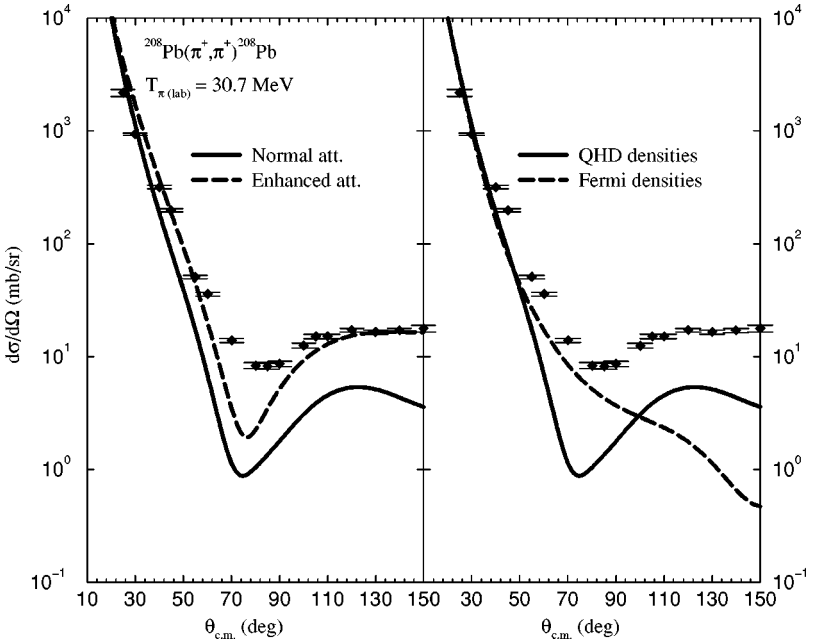

FIG. 8. The differential cross section of π^+ elastic scattering from ^{208}Pb as a function of the scattering angle in the c.m. frame at pion laboratory kinetic energy of 30.7 MeV. Experimental data are obtained from Ref. [26]. The left panel displays the results with normal (solid line) and enhanced (dashed line) *s*-wave attractions. The right panel shows the cross section with Walecka model (QHD) calculations for the nuclear densities (solid line) and with a two-parameter Fermi density (dashed line). The figure illustrates the effects of missing low-energy *s*-wave strength as well as the uncertainty arising from different calculations for the nuclear structure.

section of π^+ elastic scattering from ^{12}C at pion laboratory kinetic energy of 30.3 MeV. The experimental data, taken from Ref. [26], are well reproduced.

It is necessary here to stress one caution in comparing theoretical results with experimental data. The derived optical potential depends on the matter and isonuclear densities. These densities are independent of the reactive content of the π-nucleus interaction but depends solely on the static properties of nuclei. They can be calculated with a variety of models with different sophistication. This in turn introduces an element of ambiguity in comparing to experimental data as we cannot determine whether any discrepanices with the data are due to the optical potential or to the nuclear density calculations. In the right panel of Fig. 8, we exhibit two calculations, one using Walecka model (QHD) [25] while the other using the simple two-parameter Fermi densities [27]. It is evident that there are significant differences at large angles attributed to differences in the large momentum components of the densities in these two models. In order to minimize, if not eliminate, the ambiguities arising from nuclear densities, and in order to concentrate our investigation on the reactive content of the π-nucleus interaction, we have used the sophisticated Walecka model for calculating the nuclear structure.

Having provided an application of our optical potential at low energy, we proceed with comparisons at higher energies for a variety of nuclei. In Fig. 10 we show a comparison for

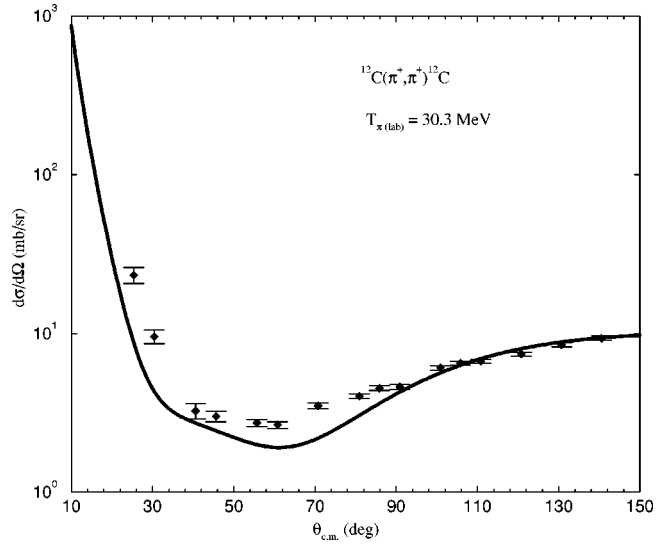

FIG. 9. The differential cross section of π^+ elastic scattering from ^{12}C as a function of the scattering angle in the c.m. frame at pion laboratory kinetic energy of 30.3 MeV. Experimental data are obtained from Ref. [26]. This figure provides an application of the optical potential at low energy.

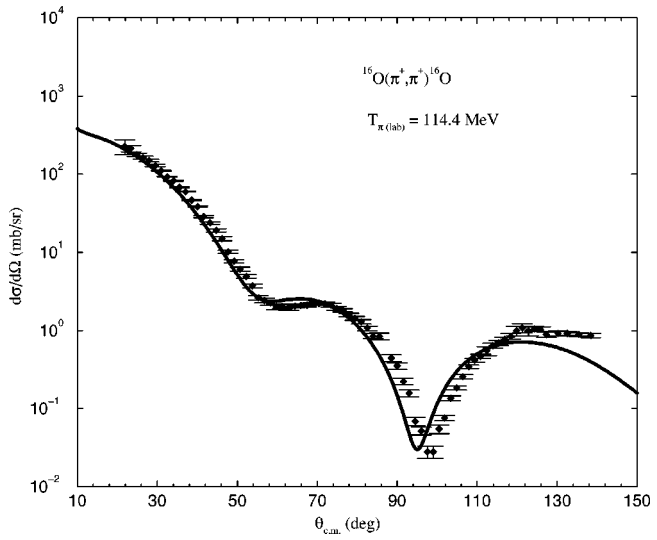

FIG. 10. The differential cross section of π^+ elastic scattering from ^{16}O as a function of the scattering angle in the c.m. frame at pion laboratory kinetic energy of 114.4 MeV. Experimental data are obtained from Ref. [28]. The figure provides an application of the optical potential at intermediate energy.

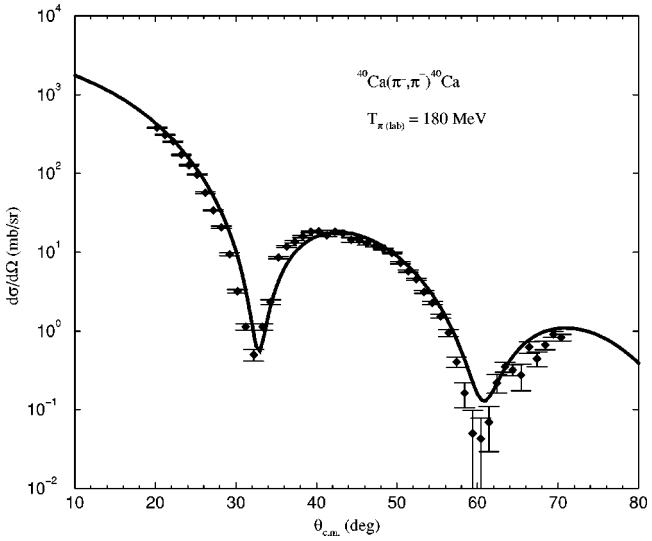

FIG. 11. The differential cross section of π^- elastic scattering from ^{40}Ca as a function of the scattering angle in the c.m. frame at pion laboratory kinetic energy of 180 MeV. Experimental data are obtained from Ref. [29]. The figure provides an application of the optical potential close to the Δ-resonance peak.

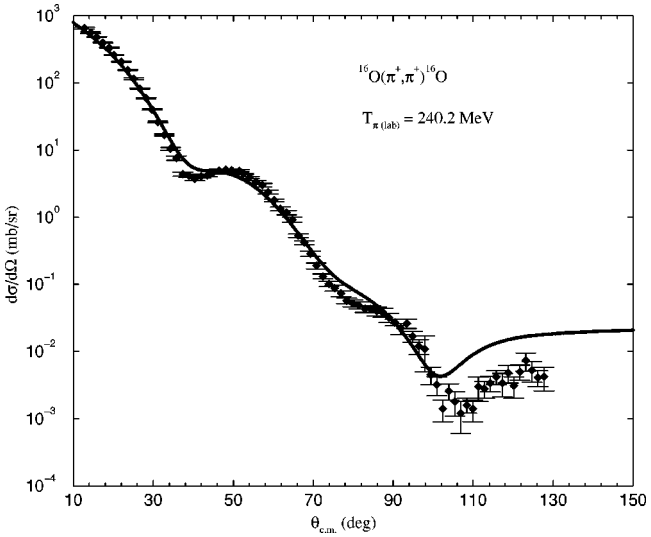

FIG. 12. The differential cross section of π^+ elastic scattering from ^{16}O as a function of the scattering angle in the c.m. frame at pion laboratory kinetic energy of 240.2 MeV. Experimental data are obtained from Ref. [28]. The figure provides an application of the optical potential towards the end of the Δ-resonance region.

^{16}O at at pion laboratory kinetic energy of 114.4 MeV, with experimental data from Ref. [28]. In Fig. 11, we exhibit the results for ^{40}Ca at laboratory kinetic energy of 180 MeV (close to the Δ-resonance peak) with data obtained from Ref. [29]. Finally in Fig. 12, we show a comparison for ^{16}O at 240.2 MeV, that is towards the end of the Δ-resonance region. The data are taken from Ref. [28]. It is evident that the experimental data are well reproduced by the inherent dynamics of the potential. One should stress here that this agreement is generated using a physics-based potential rather than a phenomenological one with free parameters to be chosen. All parameters in our treatment have their origin in the physics behind the scattering process. One in principle can modify the parameters in order to fit any specific nucleus, but we prefer this fundamental approach with its innate unity and clear conception.

V. CONCLUSIONS

In conclusion, based on an earlier seminal treatment of the low-energy π-nucleus optical potential, we have derived a potential form applicable from threshold up to the Δ-resonance region. We have done so by deriving the impulse approximation expression and then adding to it kinematical and physical corrections. The kinematical ones arise from transforming the impulse approximation expression from the π-N c.m. frame to the π-nucleus c.m. system, while the physical ones stem mostly from the many-body nature of the π-nucleus interaction. By taking advantage of experimental advances in our knowledge of the π-N process, we have updated earlier treatments with parameters calculated from state-of-the-art experimental measurements. In this manner, we provide a physics-based optical potential that can be used in diverse studies involving the π-nucleus interaction.

ACKNOWLEDGMENTS

I am very grateful to Professor J.A. Carr for the many informative discussions we have had on this subject. Furthermore, I would like to thank Professor G.C. Hillhouse for his advice on Coulomb distortions as well as Professor R.J. Peterson for supplying me with some of the experimental data. This work was supported by the Japan Society for the Promotion of Science and the United States National Science Foundation under Grant No. 0002714.

[1] A. J. Sarty *et al.* (unpublished).
[2] B. Krusche (private communication).
[3] M. Schmitz, Ph.D. thesis, Mainz 1996.
[4] G. Koch *et al.*, Phys. Rev. Lett. **63**, 498 (1989).
[5] R. W. Gothe, W. Lang, S. Klein, B. Schoch, V. Metag, H. Stroher, S. J. Hall, and R. Owens, Phys. Lett. B **355**, 59 (1995).
[6] L. J. Abu-Raddad, J. Piekarewicz, A. J. Sarty, and R. A. Rego, Phys. Rev. C **60**, 054606 (1999).
[7] L. J. Abu-Raddad, Ph.D. thesis, Florida State University, 2000; nucl-th/0005068.
[8] M. B. Johnson and D. J. Ernst, Ann. Phys. (N.Y.) **219**, 266 (1992).
[9] J. A. Carr, H. McManus, and K. Stricker, Phys. Rev. C **25**, 952 (1982).
[10] K. Stricker-Bauer, Ph.D. thesis, Michigan State University, 1980.
[11] K. Stricker, J. A. Carr, and H. McManus, Phys. Rev. C **22**, 2043 (1980).

[12] K. Stricker, H. McManus, and J. A. Carr, Phys. Rev. C **19**, 929 (1979).
[13] A. Nagl, V. Devanathan, and H. Überall, *Nuclear Pion Photoproduction*, Springer Tracts in Modern Physics Vol. 120 (Springer-Verlag, Berlin, 1991), p. 75.
[14] G. Rowe, M. Salomon, and R. H. Landau, Phys. Rev. C **18**, 584 (1978).
[15] R. A. Arndt, I. I. Strakovsky, R. L. Workman, and M. M. Pavan, Phys. Rev. C **52**, 2120 (1995).
[16] A. K. Kerman, H. McManus, and R. M. Thaler, Ann. Phys. (N.Y.) **8**, 551 (1959).
[17] L. Heller, G. E. Bohannon, and F. Tabakin, Phys. Rev. C **13**, 742 (1976).
[18] M. Ericson and T. E. O. Ericson, Ann. Phys. (N.Y.) **36**, 323 (1966).
[19] M. Krell and T. E. O. Ericson, Nucl. Phys. **B11**, 521 (1969).
[20] J. D. Jackson, *Classical Electrodynamics* (Wiley, New York, 1962), p. 119.
[21] G. Baym and G. E. Brown, Nucl. Phys. **A247**, 395 (1975).
[22] E. Oset and W. Weise, Nucl. Phys. **A319**, 477 (1979).
[23] J. Chai and D. O. Riska, Nucl. Phys. **A329**, 429 (1979).
[24] R. H. Landau and M. Mcmillan, Phys. Rev. C **8**, 2094 (1973).
[25] B. D. Serot and J. D. Walecka, Adv. Nucl. Phys. **16**, 1 (1986).
[26] B. M. Preedom *et al.*, Phys. Rev. C **23**, 1134 (1981).
[27] B. Povh, K. Rith, C. Scholz, and F. Zersche, *Particles and Nuclei: An Introduction to the Physical Concepts* (Springer, Berlin, 1995), p. 68.
[28] J. P. Albanese, J. Arvieux, J. Bolger, E. Boschitz, C. H. Q. Ingram, J. Jansen, and J. Zichy, Nucl. Phys. **A350**, 301 (1980).
[29] K. G. Boyer *et al.*, Phys. Rev. C **29**, 182 (1984).